(Received 10 July 2024, Accepted 6 August 2024, Scheduled 19 August 2024)

A Wideband High-Isolated Dual-Polarized Magnetoelectric Dipole Antenna for 4G/5G Communications

Yanhong Xu[1,*], Minling Wang[1], Xiaochao Yang[2], Can Cui[1], Xuhui Fan[1], Tingting Bai[1], and Jianqiang Hou[3]

[1] *Xi'an Key Laboratory of Network Convergence Communication, College of Communication and Information Engineering Xi'an University of Science and Technology, Xi'an 710054, China*
[2] *China Academy of Space Technology Xi'an, Xi'an 710100, China*
[3] *National Key Laboratory of Science and Technology on Antenna and Microwave, Xidian University, Xi'an 710071, China*

ABSTRACT: A highly-isolated dual-polarized magnetoelectric (ME) dipole antenna is proposed in this letter, where a modified cross-shaped differentially-feeding structure is designed to realize dual-linear polarizations (LPs). To broaden the bandwidth of the differentially-driven ME dipole antenna, a pair of L-shaped branches are loaded on the positions where a triangle is cut out of each patch to introduce a new resonant frequency at the upper frequency region. Meanwhile, a two-stepped structure is added to each of the four ports of the cross-shaped differentially-feeding structure to improve the impedance matching characteristic of the antenna. In this way, the 10 dB bandwidth is improved from 64.9% (1.54–3.02 GHz) to 83.5% (1.52–3.70 GHz), i.e., 28.7% bandwidth enhancement is achieved. A prototype is fabricated and measured. The results show that the proposed antenna can achieve a high differential port-to-port isolation of better than 38 dB, cross-polarization level (CRPL) lower than −25 dB, and peak gain up to 10.5 dBi.

1. INTRODUCTION

The rapid development of wireless technique results in the continuously increasing number of communication users, which would mean higher requirements on channel capacity and transmission rate. Since dual-polarized antennas can effectively reduce multipath fading and provide a larger channel capacity, they have been widely utilized in base stations [1]. Differentially-driven antennas are directly connected to RF integrated circuits without additional balun, which can effectively reduce the signal loss and improve the antenna efficiency [2]. Differentially-driven dual-polarized antennas also have great application prospects in base station applications due to the characteristics of high isolation and low cross-polarization. Therefore, it is of great significance to design a wideband differentially-driven dual-polarized antenna for base station applications.

Magnetic dipoles and electric dipoles are two common types of antenna elements, which exhibit complementary radiations properties [3, 4]. Based on the complementary concept, Luk and Wong proposed ME dipole antenna in 2006 [5], which has many excellent properties such as wide bandwidth, high gain, low cross-polarization level (CRPL), and stable radiation patterns. Since then, many scholars have proposed various types of wideband ME dipole antennas with different structures and radiation characteristics [6–8], but they have only one polarization. In 2008, Wu and Luk proposed a broadband dual-polarized ME dipole antenna, which was excited by two Γ-shaped strips [9]. The antenna can achieve an impedance bandwidth of 65.9%. Subsequently, many methods have been proposed for widening the bandwidth of a dual-polarized ME dipole antenna [10–15]. By modifying the feeding structures, 53.2% and 80% impedance bandwidths are achieved in [10] and [11]. Both antennas are used for 5G communication applications. In [12–14], the primary radiation structures are redesigned to achieve a wider bandwidth. Specifically, by changing the shape of the radiation structure to an octagonal loop [12], the impedance bandwidth of 68% is achieved, and the port isolation is better than 25 dB. An impedance bandwidth of 50.6% is realized, and the port isolation is higher than 45 dB by using L-shaped elements in [13]. In [15], a parasitic element and an improved feed structure are designed to achieve a wide bandwidth where an impedance bandwidth of 78.6% is achieved, and the port isolation is higher than 20 dB. Besides, ME dipole antennas have been continuously designed for different applications, such as millimeter wave applications [16, 17] and satellite communication [18]. Nevertheless, many of the above antennas have complex feeding structures.

In recent years, several differentially-driven dual-polarized antennas have been proposed in [19–23], where the port-to-port isolation can be improved by using a differentially-driven structure. In [19], the differentially-driven feeding structure is realized by two coaxial cables through a short stub, and an impedance bandwidth of 45% and a high isolation of 45 dB are achieved. In [20], the wide bandwidth is realized through two layers of stacked patches, and the differentially-feeding structure contributes to the high isolation of 35 dB. A dual-polarized ME dipole antenna with a differentially-feeding structure is proposed in [23], which realizes a bandwidth of 68%, and the

* Corresponding author: Yanhong Xu (yanhongxuxidian@163.com).

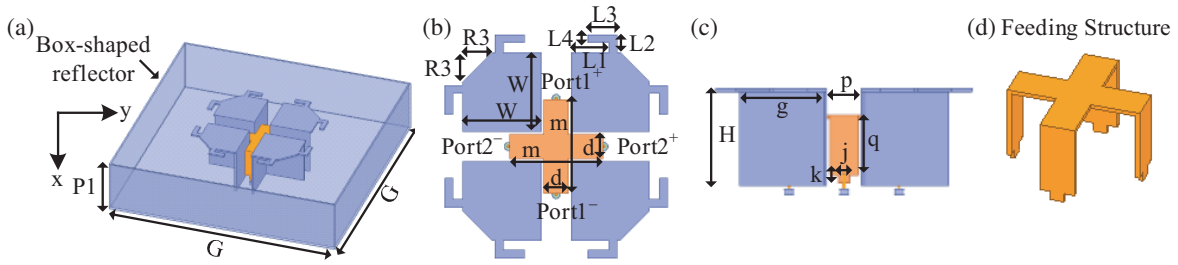

FIGURE 1. Structure of proposed ME dipole antenna. (a) Perspective view. (b) Zoomed-in top view. (c) Side view. (d) Zoomed-in view of differentially-feeding structure. ($G = 160$, $W = 29$, $H = 31$, $g = 28$, $p = 11$, $d = 9$, $q = 21.4$, $L1 = 14$, $L2 = 6.6$, $L3 = 10.8$, $L4 = 3$, $b = 11$, $k = 2.4$, $j = 3.6$, $P1 = 35$, $R3 = 10.8$ in mm).

isolation between the two ports is better than 36 dB. At present, it is still a challenge to design a dual-polarized antenna that can simultaneously achieve high isolation and wide bandwidth.

In this paper, we aim to design a dual-polarized ME dipole antenna with a wider bandwidth and a higher isolation. Inspired by the work presented in [23], this paper presents a wideband high-isolated dual-polarized ME dipole antenna. In particular, by loading a pair of L-shaped branches on each of the four-sectional structures, a new resonant frequency is introduced around 3.5 GHz. To improve the impedance matching characteristic of the antenna, a two-stepped structure is inserted into each of the four ports of the cross-shaped differentially-feeding structure. In this way, a 10 dB bandwidth of 83.5% (1.52–3.70 GHz) is achieved, i.e., 28.7% bandwidth enhancement is achieved from 64.9% (1.54–3.02 GHz) to 83.5%. The good agreement between the simulated and measured results demonstrates the excellent performance of the proposed antenna.

2. ANTENNA DESIGNS AND ANALYSIS

2.1. Theory of Differentially-Driven Dual-Polarized Antenna

For the differentially-driven dual-polarized antenna, it can be modeled as a single-ended four-port network. The single-ended ports 1 and 2 are designated as differential port 1, and the single-ended ports 3 and 4 are designated as differential port 2. The differential S-parameters are defined as [24],

$$\begin{aligned} S_{dd11} &= \frac{1}{2}\left(S_{11} - S_{21} - S_{12} + S_{22}\right) \\ S_{dd12} &= \frac{1}{2}\left(S_{13} - S_{23} - S_{14} + S_{24}\right) \\ S_{dd21} &= \frac{1}{2}\left(S_{31} - S_{41} - S_{32} + S_{42}\right) \\ S_{dd22} &= \frac{1}{2}\left(S_{33} - S_{34} - S_{43} + S_{44}\right) \end{aligned} \tag{1}$$

The differential reflection coefficients of differential ports 1 and 2 are expressed as S_{dd11} and S_{dd22}. The couplings of differential signal between differential ports are defined as S_{dd21} and S_{dd12}, where S_{mn}, $m, n = 1, 2, 3, 4$ is the single-ended S-parameters when the differentially-driven dual-polarized antenna is regarded as a single-ended four-port network. Therefore, it is expected that the coupling is very small if the differentially-driven dual-polarized antenna is composed of two identical elements. In our design, the proposed antenna is completely 90 degrees rotationally symmetrical. Thus, the following equations can be derived,

$$\begin{aligned} S_{dd11} &= S_{dd22} \\ S_{dd21} &= S_{dd12} \end{aligned} \tag{2}$$

2.2. Antenna Structure

Figures 1(a)–(d) provide the geometry of the proposed antenna. As can be observed from these Figures, the radiation structure consists of two pairs of planar electric dipoles loaded with L-shaped branches, two pairs of vertically oriented shorted patches, and a differentially-driven feeding structure. In particular, four pairs of L-shaped branches are designed to improve the operational bandwidth. A triangle with a side length of $R3$ is cut out of each planar dipole to improve the impedance matching characteristic. The differentially-driven feeding structure comprises two pairs of vertical plates and a cross-shaped horizontal plate. A two-stepped structure is inserted into each of the four ports to further improve the impedance matching. Besides, to further reduce the back radiation and increase the front-to-back ratio (FBR), a box reflector is designed.

The two lower edges of each pair of vertical parallel plates are connected to the inner conductors of a pair of 50 Ω SMA. Each pair of SMA ports is designated as a differential port of the proposed antenna. Differential port 1 consists of port 1^+ and port 1^-, while differential port 2 consists of port 2^+ and port 2^-. The differential signals with the same amplitude and 180° phase difference are transmitted to the differential ports 1 and 2, respectively. As shown in Figures 2(a)–(b), when differential port 1 is excited, the antenna is polarized along the x-direction; when differential port 2 is excited, the antenna is polarized along the y-direction.

2.3. Design Procedures

The antenna design procedure is shown in Figure 3(a). Firstly, based on the antenna in [23], the operating band is shifted to higher frequency by reducing the physical size of the antenna, and a box-shaped reflector is used in lieu of the square ground plane to improve FBR, and the resultant antenna is termed as

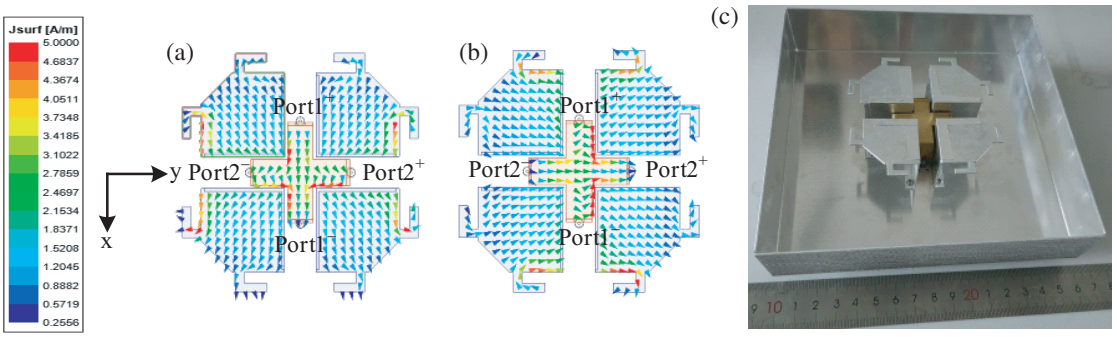

FIGURE 2. Working modes of the dual-polarized ME dipole antenna. (a) Differential port 1 is excited. (b) Differential port 2 is excited. (c) Prototype of the proposed antenna.

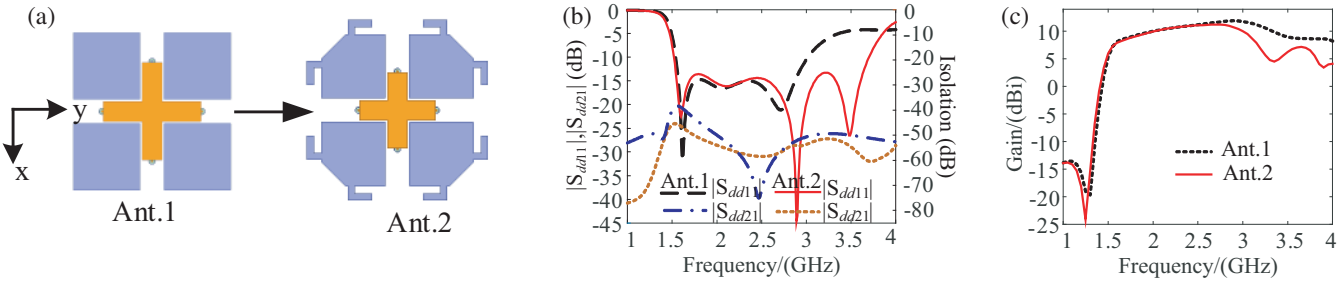

FIGURE 3. (a) Antenna design procedures. (b) Simulated $|S_{dd11}|$ and isolation of Ant. 1 and Ant. 2. (c) Simulated gains of Ant. 1 and Ant. 2.

Ant. 1 whose 10 dB bandwidth is 64.9% (1.54–3.02 GHz) as depicted from Figure 3(b). Subsequently, four pairs of L-shaped branches are loaded on the outer side of the four patch portions to introduce a new resonant frequency point. Note that these L-shaped structures are in the same size to form a symmetrical radiation pattern. Meanwhile, four triangles are cut off at the edge of the four patch sections, and a two-stepped structure is added to each of the four ports of the differential feeding structure to improve the impedance matching of the antenna. The resultant antenna is termed as Ant. 2. Figures 3(b)–(c) show the simulated differential S-parameters and gains of the above two antennas. Since the antenna structure is symmetrical, only the simulated result of differential port 1 is provided. From Figure 3(b), it can be seen that Ant. 2 exhibits a new resonance point at 3.5 GHz. The impedance bandwidth of Ant. 2 is 83.5% (1.52–3.70 GHz), which is 28.6% wider than that of Ant. 1. Meanwhile, the simulated antenna isolation is higher than 45 dB, and the peak gain is up to 11.2 dBi across the operating frequency region.

Figures 4(a)–(b) illustrate the effects of $L1$ and $L2$ on $|S_{dd11}|$, respectively. From Figure 4(a), it is seen that $L1$ has a great influence on the value of $|S_{dd11}|$ at 2.50–3.50 GHz. When $L1$ increases gradually, the impedance matching becomes worse at 2.50–3.0 GHz but better at 3.0–3.50 GHz. Finally, $L1$ is selected as 14 mm. As shown in Figure 4(b), the resonant frequency at high frequency moves toward the low-frequency band as $L2$ increases. At the same time, the impedance matching of the low frequency becomes worse. Finally, $L2$ is chosen as 6.6 mm to obtain a wide operating band with good impedance matching. Figure 4(c) shows the effects of $R3$ on $|S_{dd11}|$. It can be observed that when $R3$ is selected as 10.8 mm, a good impedance matching is achieved. To better understand the operating principle of the proposed antenna, Figure 4(d) presents the surface current distributions of the proposed antenna at 3.5 GHz when the differential ports 1 and 2 are excited, respectively. It can be observed that the current is mainly distributed around the L branches at 3.5 GHz. The entire length of a pair of L branches is around 0.41λ at 3.5 GHz.

2.4. Principle of Operation

To illustrate the working principle of the proposed antenna, Figure 4(e) shows the current distributions of the proposed antenna from differential port 1. At time $t = 0$, the currents are primarily concentrated on the electric dipole, while the currents on the magnetic dipole are the smallest. At time $t = T/4$, the currents on the electric dipole reach minimum strength, while the currents on the magnetic dipole reach maximum strength. At time $t = T/2$, the currents on the electric dipole are dominated again with opposite current direction to that at time $t = 0$. At time $t = 3T/4$, the currents on the magnetic dipole are dominated again with opposite current direction to that at time $t = T/4$. It can be explained that in a period, the electric dipole and magnetic dipole are excited simultaneously, which conforms to the working mechanism of the ME dipole antenna.

3. SIMULATED AND MEASURED RESULTS

To verify the performance of the designed antenna, a prototype is fabricated and measured. Figure 2(c) presents the prototype of the proposed ME dipole antenna. The feeding structure of the proposed antenna is made of copper, while the other parts

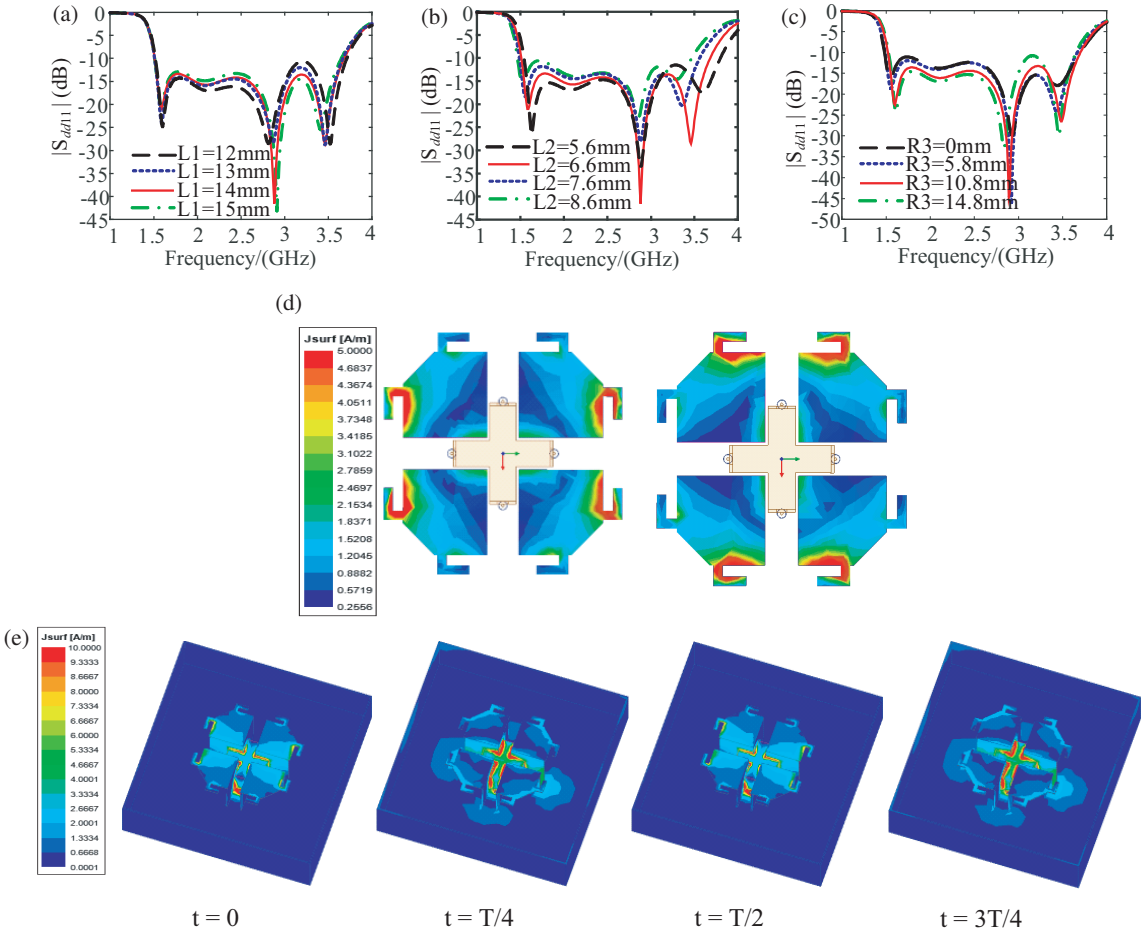

FIGURE 4. (a) Effects of $L1$ on $|S_{dd11}|$. (b) Effects of $L2$ on $|S_{dd11}|$. (c) Effects of $R3$ on $|S_{dd11}|$. (d) Current distributions of differential ports 1 and 2 excited at 3.5 GHz. (e) Current distributions of the proposed antenna from differential port 1 during a period.

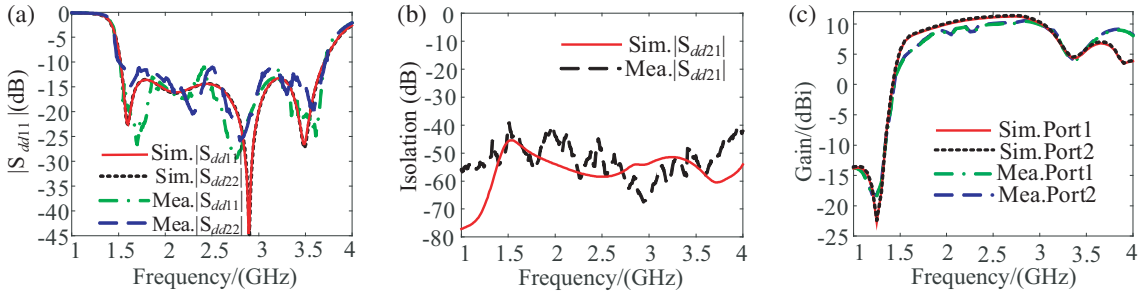

FIGURE 5. (a) Simulated and measured differential reflection coefficients at differential ports 1 and 2. (b) Simulated and measured differential isolation between two differential ports. (c) Simulated and measured antenna gains.

are made of aluminum with a thickness of 1 mm. The network analyzer is used to measure the single-ended S-parameters. After obtaining the results of the 4-port S-parameters, the measured differential S-parameters can be calculated respectively using Eq. (1). The gain and radiation patterns of the antenna are measured by a far-field measurement system. A wideband out-of-phase power divider is designed to measure the radiation characteristics of the proposed antenna [25]. When the radiation patterns of differential port 1 are measured, the two output ports of the 180° phase-shifted power divider are connected to port 1^+ and port 1^-, respectively. At the same time, port 2^+ and port 2^- are terminated with two 50 Ω loads.

Figure 5(a) provides the simulated and measured differential reflection coefficients. It can be clearly seen that there is good agreement between the simulated and measured results. Measured results show that the proposed antenna achieves an impedance bandwidth of 83.5% (1.52–3.70 GHz). The differential isolation between the two differential ports is presented in Figure 5(b), from which it can be observed that an isolation of better than 38 dB is achieved across the whole opera-

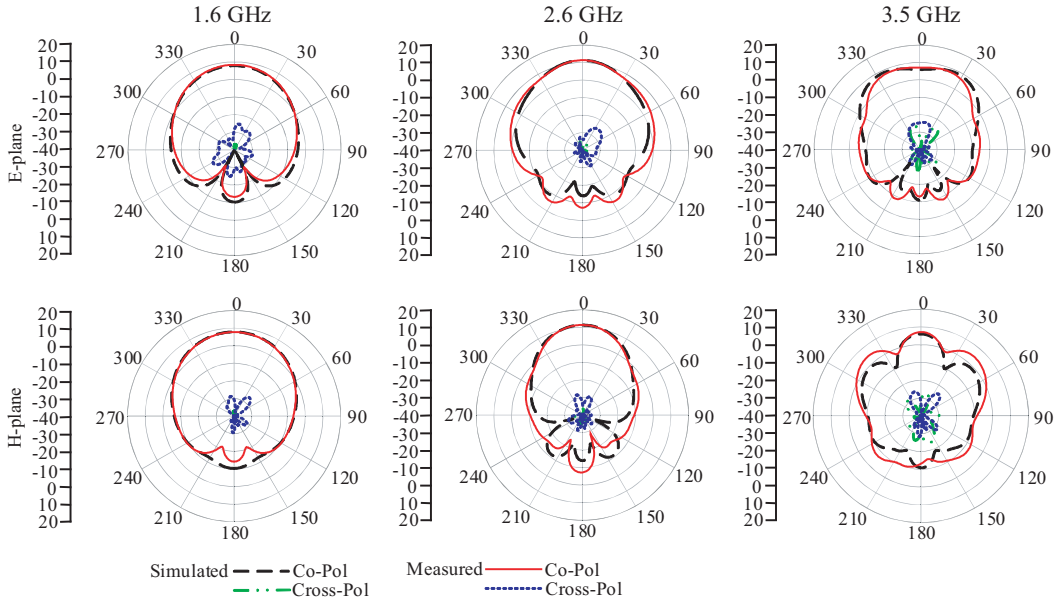

FIGURE 6. Simulated and measured radiation patterns at differential port 1.

TABLE 1. Comparison with other dual-polarized ME dipole antennas.

Ref.	Bandwidth	Isolation (dB)	CRPL (dB)	Peak gain (dBi)
[9]	65.9% (1.71–3.4 GHz)	> 36	/	9.5
[10]	53.2% (3.06–5.28 GHz)	> 22	< -19	9.6
[11]	80.0% (1.80–4.2 GHz)	> 25	/	8.5
[12]	68.0% (1.60–3.25 GHz)	> 25	< -12	9.4
[13]	50.6% (3.10–5.2 GHz)	> 45	< -18	9.8
[14]	83.0% (1.59–3.83 GHz)	> 25	< -18	10.8
[15]	78.6% (1.59–3.65 GHz)	> 20	< -15	10.4
[23]	68.0% (0.95–1.92 GHz)	> 36	< -23	9.6
Prop.	**83.5% (1.52–3.70 GHz)**	$\mathbf{> 38}$	$\mathbf{< -25}$	**10.5**

tional bandwidth. Meanwhile, the measured gains within the bandwidth range from 4.5 to 10.5 dBi, shown in Figure 5(c). Figure 6 plots the simulated and measured radiation patterns at differential port 1 of the proposed antenna at 1.6 GHz, 2.6 GHz, and 3.5 GHz. As can be seen the proposed antenna has a nearly symmetric and good unidirectional radiation pattern across the entire bandwidth. Because the aperture size becomes lager after loading the L-shaped branches, the beam width of the radiation pattern of differential port 1 becomes narrower in the H-plane at 3.5 GHz. At the same time, the CRPL of the proposed antenna is less than -25 dB, and the front-to back ratio (FBR) is greater than 14 dB across the operational frequency range.

The performance comparison of our design with other reported dual-polarized ME dipole antennas is provided in Table 1. Our goal is to design a wideband and high-isolated dual-polarized antenna for base station applications. From this table, it is clearly seen that the proposed antenna has the characteristics of wide bandwidth, high isolation, and low cross-polarization compared to previous designs.

4. CONCLUSION

This paper presents a wideband high-isolated differentially-driven dual-polarized ME dipole antenna. By loading a pair of L-shaped branches on each edge of the horizontal patches, a bandwidth of 83.5% is achieved. Using a modified feeding structure improves the isolation and reduces the cross polarization. The proposed antenna can achieve a high differential port-to-port isolation of better than 38 dB. Additionally, the proposed ME dipole antenna exhibits many excellent properties, such as high gain, low CRPL, and high FBR, which make it a good candidate for 4G and 5G base station applications.

ACKNOWLEDGEMENT

The authors would thank the editors and the anonymous reviewers for their efforts in evaluating our manuscript.

This work was supported in part by the National Natural Science Foundation of China, Grants 62271386, 62301415, and 62301414, and in part by the Shaanxi Science and Technology Association Youth Talent Lifting Program, Grant 20230149.

REFERENCES

[1] Guo, Y.-X., K.-M. Luk, and K.-F. Lee, "Broadband dual polarization patch element for cellular-phone base stations," *IEEE Transactions on Antennas and Propagation*, Vol. 50, No. 2, 251–253, 2002.

[2] Jin, H., G. Q. Luo, W. Che, K.-S. Chin, Y. Pan, and Y. Yu, "Vertically-integrated differential filtering patch antenna excited by a balun bandpass filter," *IET Microwaves, Antennas & Propagation*, Vol. 13, No. 3, 300–304, 2019.

[3] Chlavin, A., "A new antenna feed having equal E- and H-plane patterns," *Transactions of the IRE Professional Group on Antennas and Propagation*, Vol. 2, No. 3, 113–119, 1954.

[4] Clavin, A., D. Huebner, and F. Kilburg, "An improved element for use in array antennas," *IEEE Transactions on Antennas and Propagation*, Vol. 22, No. 4, 521–526, 1974.

[5] Luk, K.-M. and H. Wong, "A new wideband unidirectional antenna element," *International Journal of Microwave and Optical Technology*, Vol. 1, No. 1, 35–44, 2006.

[6] Wang, M., H. Yang, N. Hu, W. Xie, Y. Mo, Z. Chen, Z. Liu, and Z. Chen, "A novel wideband beam reconfigurable magneto-electric dipole patch antenna," *Progress In Electromagnetics Research C*, Vol. 109, 111–124, 2021.

[7] Fang, H., J. Sun, H. Zhang, Y. Liu, and Z. Wang, "Design of a wideband ME dipole antenna with wide beamwidth," *Progress In Electromagnetics Research C*, Vol. 120, 243–252, 2022.

[8] Zhang, C. Q. and L. Y. Feng, "Design of high-gain magneto-electric dipole antenna by loading a magneto-electric dipole director," *IEEE Antennas and Wireless Propagation Letters*, Vol. 22, No. 8, 1823–1827, 2023.

[9] Wu, B. Q. and K.-M. Luk, "A broadband dual-polarized magneto-electric dipole antenna with simple feeds," *IEEE Antennas and Wireless Propagation Letters*, Vol. 8, 60–63, 2008.

[10] Wu, S. and F. Shang, "Broadband dual-polarized magnetoelectric dipole antenna with compact structure for 5G base station," *IEEE Access*, Vol. 11, 20 806–20 813, 2023.

[11] Park, S. and S. Kim, "A coupled-fed broadband dual-polarized magnetoelectric dipole antenna for WLAN and sub-6 GHz 5G communication applications," *Journal of Electromagnetic Engineering and Science*, Vol. 23, No. 1, 75–77, 2023.

[12] Li, Z., Y. Sun, M. Yang, P. Tang, and Z. Wu, "A compact dual-polarized magneto-electric dipole antenna for 2G/3G/LTE applications," in *2017 Progress in Electromagnetics Research Symposium-fall (PIERS-Fall)*, 1338–1344, Singapore, 2017.

[13] Yang, M. and J. Zhou, "A broadband high-isolation dual-polarized antenna for 5G application," *Progress In Electromagnetics Research M*, Vol. 85, 39–48, 2019.

[14] Lu, Z., Y. Sun, H. Zhu, and F. Huang, "A broadband $\pm 45^\circ$ dual-polarized magneto-electric dipole antenna for 2G/3G/LTE/5G/WiMAX applications," *Progress In Electromagnetics Research C*, Vol. 86, 153–165, 2018.

[15] Zhao, L., H. Zhu, H. Zhao, G. Liu, K. Wang, J. Mou, W. Zhang, and J. Li, "Design of wideband dual-polarized ME dipole antenna with parasitic elements and improved feed structure," *IEEE Antennas and Wireless Propagation Letters*, Vol. 22, No. 1, 174–178, 2022.

[16] Dai, X., A. Li, and K. M. Luk, "A wideband compact magnetoelectric dipole antenna fed by SICL for millimeter wave applications," *IEEE Transactions on Antennas and Propagation*, Vol. 69, No. 9, 5278–5285, 2021.

[17] Xiao, Z., Y. Pan, X. Liu, and K. W. Leung, "A wideband magnetoelectric dipole antenna with wide beamwidth for millimeter-wave applications," *IEEE Antennas and Wireless Propagation Letters*, Vol. 22, No. 4, 918–922, 2022.

[18] Wu, F., J. Wang, Y. Zhang, W. Hong, and K.-M. Luk, "A broadband circularly polarized reflectarray with magneto-electric dipole elements," *IEEE Transactions on Antennas and Propagation*, Vol. 69, No. 10, 7005–7010, 2021.

[19] Cui, Y., X. Gao, and R. Li, "A broadband differentially fed dual-polarized planar antenna," *IEEE Transactions on Antennas and Propagation*, Vol. 65, No. 6, 3231–3234, 2017.

[20] Yang, X., L. Ge, and J. Wang, "A differentially driven dual-polarized high-gain stacked patch antenna," *IEEE Antennas and Wireless Propagation Letters*, Vol. 17, No. 7, 1181–1185, 2018.

[21] Xie, J.-J. and Z. Chen, "Differentially fed dual-polarized SIW cavity-backed patch antenna with wide bandwidth under multimode resonance," *Progress In Electromagnetics Research C*, Vol. 105, 229–240, 2020.

[22] Wen, D.-L., D.-Z. Zheng, and Q.-X. Chu, "A wideband differentially fed dual-polarized antenna with stable radiation pattern for base stations," *IEEE Transactions on Antennas and Propagation*, Vol. 65, No. 5, 2248–2255, 2017.

[23] Xue, Q., S. W. Liao, and J. H. Xu, "A differentially-driven dual-polarized magneto-electric dipole antenna," *IEEE Transactions on Antennas and Propagation*, Vol. 61, No. 1, 425–430, 2012.

[24] Eisenstadt, W., R. Stengel, and B. Thompson, *Microwave Differential Circuit Design Using Mixed Mode S-parameters*, Vol. 42, 1–25, Artech, Boston, MA, 2006.

[25] Zhang, Z.-Y., Y.-X. Guo, L. C. Ong, and M. Y. W. Chia, "A new wide-band planar balun on a single-layer PCB," *IEEE Microwave and Wireless Components Letters*, Vol. 15, No. 6, 416–418, 2005.